

Impact of the dominant large-scale teleconnections on winter temperature variability over East Asia

Young-Kwon Lim¹ and Hae-Dong Kim²

Received 10 November 2012; revised 29 April 2013; accepted 1 May 2013; published 31 July 2013.

[1] Monthly mean geopotential height for the past 33 DJF seasons archived in Modern Era Retrospective analysis for Research and Applications reanalysis is decomposed into the large-scale teleconnection patterns to explain their impacts on winter temperature variability over East Asia. Following Arctic Oscillation (AO) that explains the largest variance, East Atlantic/West Russia (EA/WR), West Pacific (WP) and El Niño–Southern Oscillation (ENSO) are identified as the first four leading modes that significantly explain East Asian winter temperature variation. While the northern part of East Asia north of 50°N is prevailed by AO and EA/WR impacts, temperature in the midlatitudes (30°N–50°N), which include Mongolia, northeastern China, Shandong area, Korea, and Japan, is influenced by combined effect of the four leading teleconnections. ENSO impact on average over 33 winters is relatively weaker than the impact of the other three teleconnections. WP impact, which has received less attention than ENSO in earlier studies, characterizes winter temperatures over Korea, Japan, and central to southern China region south of 30°N mainly by advective process from the Pacific. Upper level wave activity fluxes reveal that, for the AO case, the height and circulation anomalies affecting midlatitude East Asian winter temperature is mainly located at higher latitudes north of East Asia. Distribution of the fluxes also explains that the stationary wave train associated with EA/WR propagates southeastward from the western Russia, affecting the East Asian winter temperature. Investigation on the impact of each teleconnection for the selected years reveals that the most dominant teleconnection over East Asia is not the same at all years, indicating a great deal of interannual variability. Comparison in temperature anomaly distributions between observation and temperature anomaly constructed using the combined effect of four leading teleconnections clearly show a reasonable consistency between them, demonstrating that the seasonal winter temperature distributions over East Asia are substantially explained by these four large-scale circulation impacts.

Citation: Lim, Y.-K., and H.-D. Kim (2013), Impact of the dominant large-scale teleconnections on winter temperature variability over East Asia, *J. Geophys. Res. Atmos.*, 118, 7835–7848, doi:10.1002/jgrd.50462.

1. Introduction

[2] Planetary scale pattern of mass (e.g., pressure and height) and circulation anomalies that persists for a certain period, so-called “teleconnection pattern,” is known to significantly contribute to the atmospheric circulation system [Barnston and Livezey, 1987]. Such teleconnection patterns usually last from a couple of weeks to months, playing a role in determining warm or cold seasons over the vast geographical basin. Their impact on atmospheric circulation often leads to changes in temperature, precipitation, upper

tropospheric jet streams, and storm tracks, resulting in abnormal weather/climates. Improved understanding on the role of various large-scale teleconnections is very important, in that it will eventually lead to the improvement of seasonal predictive skills for the regional and/or global climate.

[3] Numerous studies have identified that El Niño–Southern Oscillation (ENSO) is almost the most important factor for determining the global seasonal climate. The response to the anomalous sea surface temperature (SST) along the central to eastern tropical Pacific alters the extra-tropical circulation structures via planetary scale wave propagation [Horel and Wallace, 1981; Barnston et al., 1991]. Thus, earlier seasonal forecasts for the extra-tropical region have mainly relied on ENSO phase [Gershunov and Barnett, 1998; Higgins et al., 2002; Meehl et al., 2007]. In recent years, there are also increasing numbers of studies focusing on North Atlantic Oscillation (NAO) and Arctic Oscillation (AO) due to their strong influence on boreal winter climates [Griffiths and Bradley, 2007; L’Heureux et al., 2010; Lim and Schubert, 2011]. These studies argue the relatively weak role of ENSO

¹NASA Goddard Space Flight Center, Goddard Earth Sciences Technology and Research (GESTAR), I. M. System Group, Columbia, Maryland, USA.

²College of Environment, Keimyung University, Daegu, South Korea.

Corresponding author: H.-D. Kim, College of Environment, Keimyung University, Daegu, South Korea. (khd@kmu.ac.kr)

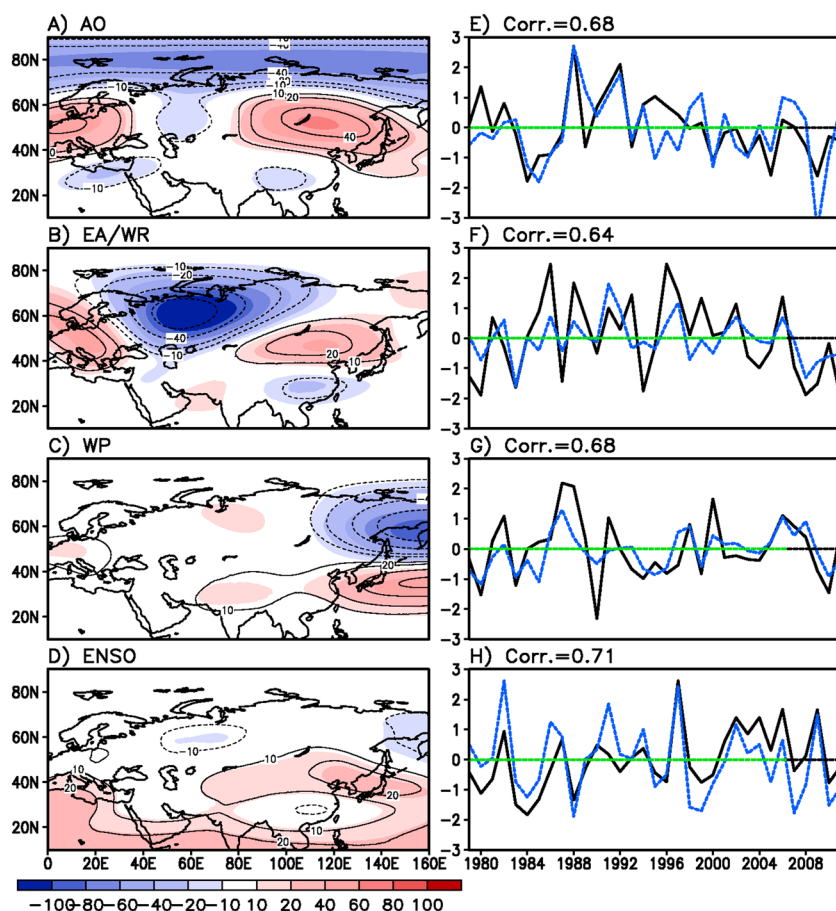


Figure 1. The first four rotated empirical orthogonal functions (REOFs) of the monthly 250 hPa height archived from MERRA reanalysis. The data set consists of data for 33 winters from 1979/1980 DJF through 2011/2012 DJF. Shaded in the left panel represents the distribution of nonnormalized eigenvectors [m], whereas the (solid line) right panel the corresponding PC time series. Dashed lines denote the teleconnection indices time series archived at NOAA/NCEP/CPC. Superimposed contours in the left panel are the REOFs extracted for the entire Northern hemispheric domain shown in Figure 2.

in recent years compared to NAO and AO, especially for eastern North America [L'Heureux *et al.*, 2010] and midlatitude to high latitudes of Asia. Griffiths and Bradley [2007] and Lim and Schubert [2011] found that the extreme weather/climate characteristics in recent winters are more controlled by NAO and AO phase for the eastern United States. Park *et al.* [2011] concludes, for the East Asian region, that AO impact has frequently caused extreme cold surges in recent winters.

[4] Since teleconnection patterns, including ENSO, are understood to explain large portions of anomalous weather/climate patterns, a complete understanding of their contribution to the climate system is very important. However, despite the identification of approximately ~ 10 prominent teleconnections [Horel, 1981; Barnston and Livezey, 1987; Washington *et al.*, 2000], we are still not capable of clearly identifying the contribution of individual teleconnection patterns to seasonal climate. For instance, there has been disparity in conclusions regarding the ENSO impact on the East Asian winter climates [Zhang *et al.*, 1997; Chen *et al.*, 2004]. Few studies have intensively evaluated the relative importance between AO and ENSO for the East Asian region, while there are a small number of studies on such issues for North America. Whether the winter climate over East Asia is mostly explained by these

two teleconnections (AO and ENSO) is also not clear. Wang *et al.* [2011] discusses that East Atlantic/West Russia (EA/WR) teleconnection pattern [Barnston and Livezey, 1987; Washington *et al.*, 2000], which originated in the Atlantic, is influential to modulate the Asian winter monsoon. However, compared with numerous studies on the relatively well-known AO and ENSO, the impact of EA/WR and its importance for the East Asian winter climate has not attracted any significant and detailed investigation. The impacts of West Pacific (WP) [Mo and Livezey, 1986; Linkin and Nigam, 2008] and Pacific North American teleconnection patterns also need clarification due to their origin in the Pacific, where the associated atmospheric structures might play a role in determining the winter climate over East Asia.

[5] The present study is motivated by these unresolved questions on the impact of teleconnection patterns and ENSO on determining the winter climate over East Asia. In this study, we first identify the dominant teleconnection patterns that substantially explain the East Asian winter temperature characteristics. We then investigate the various atmospheric structures which are physically linked to each teleconnection to explain dominant physical processes affecting East Asian winter temperatures. The degree of

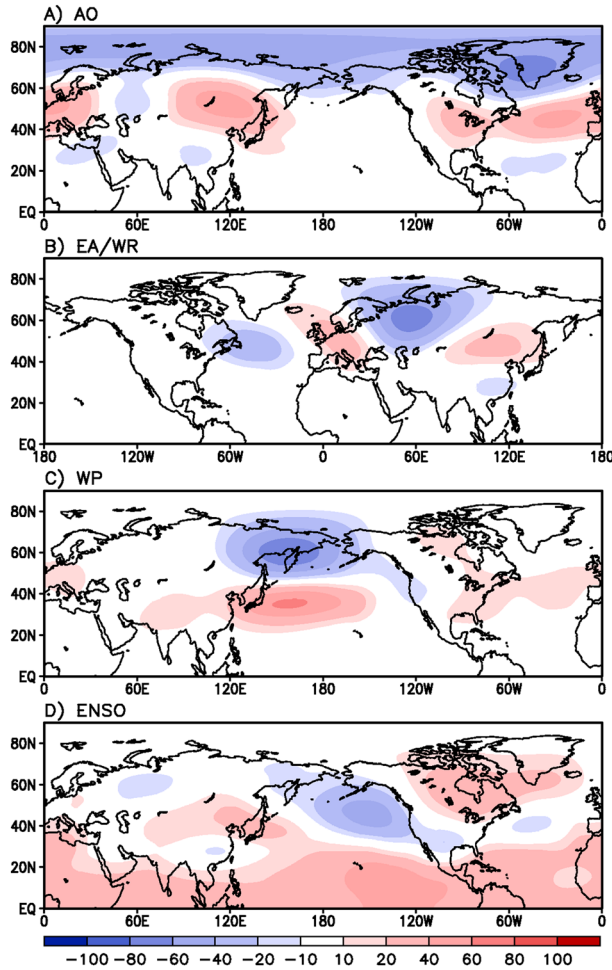


Figure 2. Same as Figure 1, but for the expanded domain covering the entire Northern Hemisphere.

contribution of each teleconnection to the East Asian winter temperature is also compared. We believe that the present study significantly advances our understanding of the impact of large-scale teleconnections, as previous studies have conventionally focused on either one of AO or ENSO.

[6] Section 2 describes the data which have been utilized in this study. Identification of the leading teleconnection patterns that explain the temperature variability over Asia is described in section 3. Sections 4 and 5 delineate the correlated patterns and regressed atmospheric structures resulting from the impact of leading large-scale teleconnections. Wave activity flux patterns are also investigated to identify the source and propagation of large-scale stationary waves associated with teleconnections. Section 6 investigates the interannual change in the contribution of teleconnection to East Asian winter temperature and is followed by concluding remarks and discussion in section 7.

2. Data

[7] Modern Era Retrospective analysis for Research and Applications (MERRA) reanalysis data [Rienecker et al., 2011] that was produced with the NASA Goddard Earth Observing System Data Assimilation System Version 5 are used for the past 33 winters from 1979/1980 DJF (December,

January, and February) through 2011/12 DJF. The variables primarily utilized are upper level (250 and 300 hPa) geopotential height, wind (300 and 850 hPa), temperature (300, 850 hPa, and 2 m level), and sea level pressure. Their horizontal resolution is 0.5° latitude \times 0.6667° longitude, and daily data are taken as averages over a month in order to create monthly mean data.

3. Identification of the Leading Teleconnection Patterns Affecting the East Asian Winter Temperature

[8] Upper level (250 hPa) geopotential height is used for capturing the large-scale teleconnections that significantly explain the East Asian winter temperature variability. The 250 hPa pressure level is selected because the 250 hPa height is understood to explain well the large-scale mass distribution linked to the polar jet stream typically located near the 250–300 hPa level in winter. We removed the monthly climatological cycle for the DJF season and then applied the Rotated Empirical Orthogonal Function (REOF) technique. Four leading teleconnection patterns were identified within the past 33 winter periods (Figure 1). Captured patterns, in decreasing order of variance for the domain in Figure 1, are AO [Thompson and Wallace, 1998] (12.8%), EA/WR [Barnston and Livezey, 1987; Washington et al., 2000; Wang et al., 2011] (12.7%), WP [Mo and Livezey, 1986; Linkin and Nigam, 2008] (7.1%), and ENSO (6.8%). The left panel in Figure 1 (shaded) depicts their spatial patterns, while the corresponding principal component (PC) time series are plotted on the right panel. Dashed lines on the right panel represent the time series of the individual teleconnection indices archived at the National Oceanic and Atmospheric Administration (NOAA)/National Center for Environmental Prediction (NCEP)/Climate Prediction Center (CPC) (ftp://ftp.cpc.ncep.noaa.gov/wd52dg/data/indices/tele_index.nh). The identified PC time series and index time series are in good agreement, confirming the reliable capture of leading teleconnection patterns by REOF. Note that all spatial patterns and PC time series are plotted on a positive phase basis.

[9] As established by many previous studies, the AO pattern in Figure 1a represents the zonally symmetric alternating pattern between geopotential height (and sea level pressure) in the Arctic and the Northern Hemispheric midlatitudes [Thompson and Wallace, 1998]. The positive height anomaly which occurs over East Asia during the positive phase favors an easterly anomaly crossing the southern part of Japan and Korea. Low level (850 hPa) also exhibits an easterly anomaly over this region as can be viewed in detail in Figure 5a. Figure 1a with an opposite sign, which would correspond to the negative AO phase, indicates that the easterly anomaly from the Pacific is expected toward the Asian continent at around 60°N . Over midlatitude East Asia (30°N – 40°N), a westerly anomaly that might transport a continental cold air mass would be dominant during the negative phase.

[10] The EA/WR pattern is understood to have two large-scale anomaly centers located near the Caspian Sea and western Europe, influencing Eurasian climates [Barnston and Livezey, 1987]. EA/WR then propagates farther eastward and spans continental midlatitude Asia (Figure 1b) [Washington et al., 2000], as it is discussed in detail in Figure 9b. During the positive EA/WR phase, the positive height anomaly is observed over East Asia north of 40°N ,

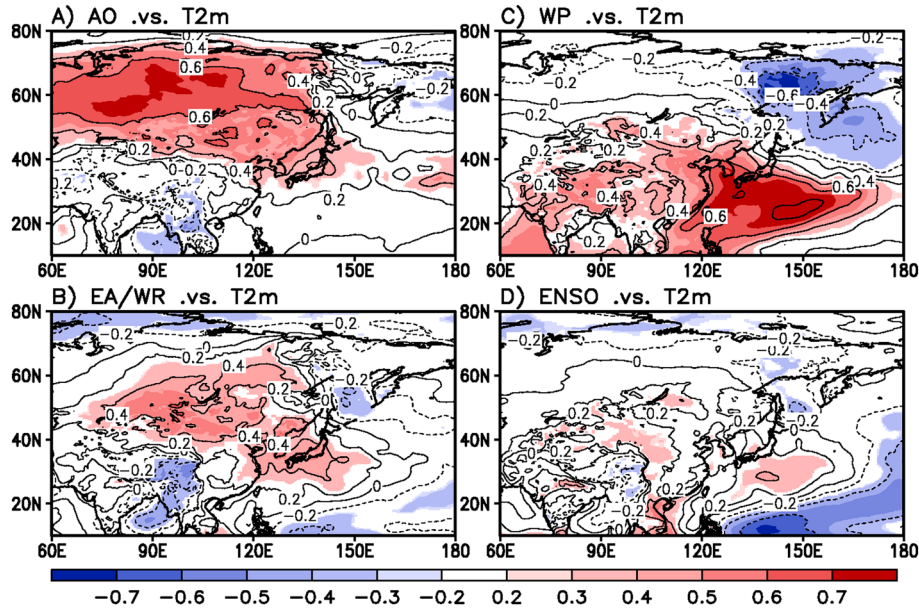


Figure 3. Correlations between the first four leading teleconnection indices and seasonal mean 2 m air temperatures. Values are detrended before computing the correlations. Correlations statistically significant at 10% level are shaded.

while the negative anomaly is found south of this point (Figure 1b). Anticyclonic circulation in conjunction with the easterly anomaly from the Pacific is possible along 35°N–40°N during the positive EA/WR phase, whereas cyclonic circulation with the westerly anomaly from inland will be dominant during the negative phase.

[11] The WP pattern in Figure 1c has been reported to have a great potential to influence the winter climate variability over the Pacific [Linkin and Nigam, 2008]. The pattern consists of a north-south dipole of anomalies, reflecting variations in the location and strength of the jet stream over East Asia [Wallace and Gutzler, 1981; Barnston and Livezey, 1987]. WP can be also understood as the basin analog of the North Atlantic Oscillation (NAO), as both construct a north-south dipole structure, perturb the climatological jet, and are connected to storm track modulation [Linkin and Nigam, 2008]. The well-known ENSO mode (see consistency between ENSO mode PCs and Niño3.4 index in Figure 1h) in Figure 1d shows that the El Niño impact constructs the positive height anomaly over the East Asian midlatitudes (30°N–50°N), while a negative anomaly will be dominant over the region during the La Niña phase.

[12] In order to clarify that the four patterns in Figure 1 are robust, we repeat the modal separation by expanding the domain covering the entire Northern Hemisphere. This calculation provides a global scale distribution of the individual teleconnections. Figure 2 demonstrates that the four major patterns presented in Figure 1 are stable and robust. For clearer verification of robustness, the patterns for the Eurasian region in Figure 2 are superimposed by contours in Figure 1. Particularly, Figures 2b–2d imply the possible connectivity of the East Asian winter temperature to the patterns over the remote regions, which are midlatitude Atlantic for EA/WR (Figure 2b), midlatitude to high-latitude western Pacific for WP (Figure 2c), and central to eastern tropical Pacific for ENSO (Figure 2d).

4. Correlated Structure Between Temperature and Teleconnection

[13] We evaluated the linear relationship between the interannual variation of leading large-scale teleconnections and the 2 m air temperature. Correlations are calculated between the index of each teleconnection and the climatology-removed 2 m air temperature. Figure 3 shows the positive correlation with temperature over East Asia, implying above (below) average temperature connected with the positive (negative) teleconnection phase.

[14] Figure 3a represents that AO is the most dominant teleconnection pattern for the Eurasia region (corr. = 0.6–0.8). The impact of AO reaches to the East Asian midlatitudes, including northeastern China, Korea, and Japan (corr. = 0.4–0.6). It is known that Atlantic teleconnection patterns, such as EA/WR, play a substantial role in determining winter climates over Europe [Washington et al., 2000; Bojariu and Reverdin, 2002]. As well as this impact over Europe, EA/WR shows the relationship with the East Asian temperature variation (Figure 3b). While negative correlations (i.e., cold temperature anomalies) are found over the Arctic region, East Asia is characterized by positive correlation that indicates warm winter during positive EA/WR and cold winter during negative EA/WR phase (corr. = 0.4–0.6) (Figure 3b). WP in Figure 3c has strong positive correlation over the subtropical to midlatitudes of the western Pacific and negative correlation over the high-latitude Pacific. Such positive correlations are also observed over the continental areas of East Asia, including China south of 50°N, Korea, and Japan. Specifically, the correlations over the southern part of Korea, Japan, and Taiwan exceed 0.7, which is greater than correlations with the other three teleconnections for this region. Specific features of the ENSO-related correlations in Figure 3d include El Niño warming and La Niña cooling over East Asia. The correlation values remain near the statistical significance limit at 10%,

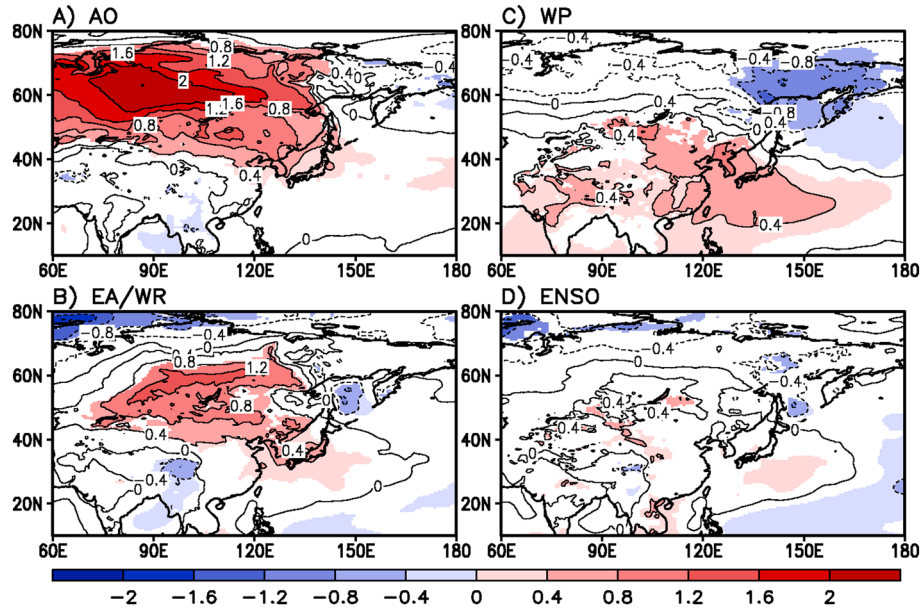


Figure 4. Distribution of the regressed 2 m air temperature anomalies [K] onto each teleconnection. Temperatures statistically significant at 10% level are shaded.

indicating that East Asian winter temperatures may be more related to AO, EA/WR, and WP than to ENSO. Recent studies also suggest that AO appears to be more influential than ENSO toward boreal winter climate variability [L'Heureux *et al.*, 2010; Park *et al.*, 2011; Lim and Schubert, 2011].

5. Temperature Anomalies and Atmospheric Circulations Linked to Each Teleconnection

[15] Regression analysis was performed to identify patterns of temperature anomalies and atmospheric circulations which are linked to teleconnections. First, the regressed 2 m air temperatures are calculated by regressing the raw temperature anomalies onto each teleconnection index (for AO, EA/WR, and WP) or Niño3.4 SST index (for ENSO) to quantify the actual temperature anomalies derived by the impact of each teleconnection. Figure 4a represents that the Eurasia region is predominantly influenced by the AO impact. Central Siberia, centered at around 90°E and 60°N, shows the strongest response to AO, with the positive (negative) AO giving rise to temperature rise (drop) more than 2 K. For the East Asia region, temperature anomalies affected by AO are primarily found all areas north of 40°N and limited areas south of 40°N that include Korea, Japan, and the Shandong peninsula in China. The magnitude of temperature anomalies greater than 1 K tends to be found north of 45°N. In contrast, the AO impact over the southern part of domains such as the area south of Shandong (~35°N) is generally very weak, as the magnitude of temperature anomalies are almost negligible over the region (Figure 4a).

[16] Temperature anomalies by the impact of EA/WR are shown in Figure 4b. It turns out that the magnitude of the impact of EA/WR on temperature over East Asia is generally smaller than that of AO, but greater than that of ENSO. Northern China, Mongolia, and Russia near Lake Baikal show a strong positive temperature response to the positive EA/WR and negative response to the negative EA/WR. The

Russian region near Lake Baikal tends to be more strongly influenced by EA/WR than other East Asian regions, as the magnitude of the temperature anomaly exceeds 1.2 K. Like AO, the EA/WR impact spans Korea and Japan, but the impact is relatively weaker than the impact over higher latitudes (i.e., north of 40°N).

[17] The WP impact in Figure 4c spans most of mainland China, Korea, and Japan and appears to explain large portions of temperature anomalies for central to southern China. The WP impact also reaches Mongolia and some southern part of Russia. In contrast, the effect of WP over high-latitude Russia, approximately north of 60°N, is opposed to that for midlatitude East Asia. These temperature anomaly distributions are strongly linked to the meridional dipole structure of pressure anomaly over the western Pacific [Linkin and Nigam, 2008].

[18] Figure 4d shows the temperature anomalies according to the impact of El Niño. The positive impact reaches East Asia, but tends to be generally weaker than the impacts of three other teleconnections. Many grid points in East Asia show temperature anomalies lower than 0.4 K, which does not satisfy the statistical significance at 10%.

[19] Atmospheric circulation at low level (850 hPa) and sea level pressure distribution, as linked to the individual teleconnections, are plotted in Figure 5. Zonal and meridional winds at the 850 hPa level and at sea level pressure are regressed onto each teleconnection index or onto the Niño3.4 SST index. Regressed distributions in Figure 5 explain that easterly or southerly flows are dominant over East Asia during the positive phase of each teleconnection. Positive sea level pressure anomalies tend to develop over the Pacific, providing favorable conditions for easterly warm flows toward East Asia. Figure 5a shows that strong negative pressure and a height anomaly in the Arctic, in conjunction with the positive anomaly in the midlatitudes, facilitate the formation of an anticyclonic circulation anomaly in the midlatitude Pacific (Figure 5a). Easterly anomalies toward

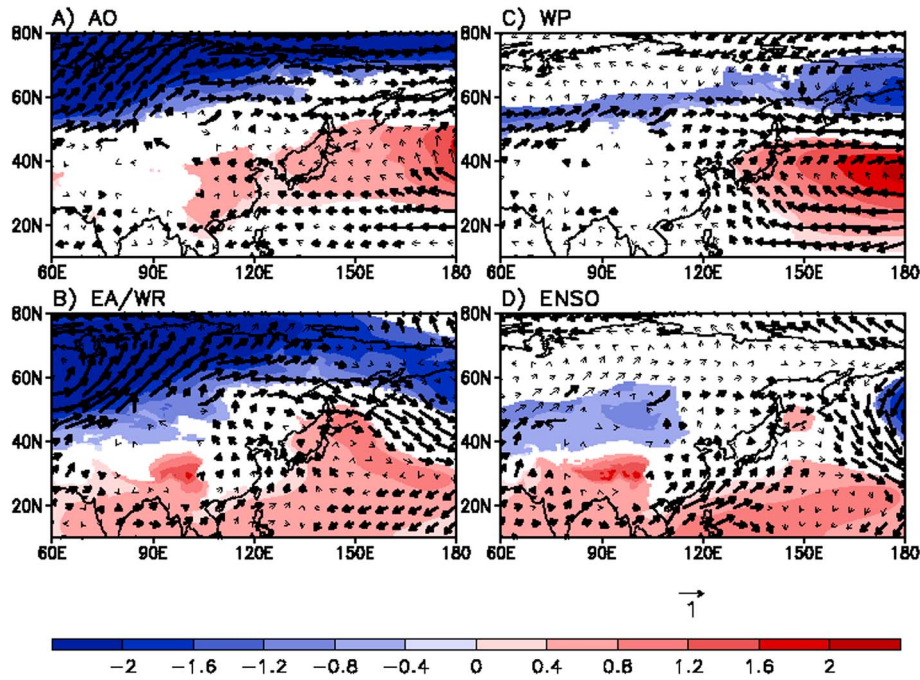


Figure 5. Distribution of the regressed 850 hPa winds [m s^{-1}] and sea level pressures [hPa] onto each teleconnection. Shaded are the regions where sea level pressure anomalies are significant at 10% level. Wind vectors statistically significant at 10% level are plotted thick.

the East Asian continent is feasible from the Pacific at 20°N–40°N (Figure 5a). In contrast, cold cyclonic flows from higher latitude regions in the Pacific (~60°N) toward East Asia are possible during the negative AO phase [Park *et al.*, 2011].

[20] For the positive EA/WR case, a large-scale negative pressure anomaly over western Russia (60°E, 60°N) results in a strong southwesterly along the southern border of the negative pressure anomaly (Figure 5b). This wind pattern is connected with the large-scale anticyclonic circulation over East Asia and the western Pacific, where a positive pressure anomaly dominates (Figure 5b). The southerly wind anomaly from the Pacific in response to this pressure distribution has a great potential to transport warm air toward China, Korea, and Japan. Atmospheric circulation anomalies for the negative EA/WR case can be understood to operate in an opposite manner. A northerly flow anomaly as a result of the large-scale cyclonic flow over East Asia may transport cold air mass toward the region.

[21] Atmospheric circulation structures due to the positive WP and El Niño also result in a warm atmospheric flow toward East Asia from the Pacific. A strong positive pressure anomaly in the midlatitude Pacific is linked to a positive WP (Figures 1c and 2c), which favors a southerly flow toward East Asia (Figure 5c). The positive sea level pressure anomalies in the tropical western Pacific in Figure 5d are connected with the anomalous Walker circulation in response to El Niño forcing. The positive pressure anomaly pattern in the western Pacific is responsible for the southerly flow that supplies the warm air mass to the East Asian continent. It should be pointed out that the wind vectors around midlatitude East Asia (China, Korea, and Japan) appears to be generally stronger in the WP and ENSO cases than in the AO case. It indicates that the role of temperature

advection by low-level atmospheric winds would be very important in the case of WP and ENSO, so as to account for the temperature distribution over East Asia.

[22] We further examined the temperature advection in Figure 6. Advective temperature change arising from the circulation linked to each teleconnection is calculated by $-V_{\text{Tel}} \times \nabla T_{\text{Cli}}$. V_{Tel} indicates the horizontal winds linked to each teleconnection, and T_{Cli} represents the climatological temperatures. Note that the contribution of the nonlinear component, $-V_{\text{Tel}} \cdot \nabla T_{\text{Tel}}$ and the other linear component, $-V_{\text{Cli}} \cdot \nabla T_{\text{Tel}}$ is negligibly small. Figure 6 shows the advective temperature changes over East Asia during the positive phase of each teleconnection. Figure 6a shows that the contribution of advection over East Asia, including northeast China, Korea, and Japan, is generally weaker in for AO than for the other three teleconnections. This implies that in the case of AO, temperature anomalies might be better explained based on their additional impacts, such as radiative impact (e.g., increase/decrease in surface shortwave radiation) [Linkin and Nigam, 2008]. Temperature distributions for positive EA/WR, WP, and ENSO show a wide area of warm temperature advection over the western Pacific as well as the continental area of East Asia (Figures 6b–6d). As discussed in Figure 5, well-developed southerly flows at low atmospheric levels substantially contribute to the transport of warm air toward East Asia. For example, advective temperature changes during the ENSO episode are greater than those in the AO case (Figure 6d), indicating that a large portion of the temperature anomalies associated with ENSO can be explained by temperature advection.

[23] Temperature changes for the case of negative phase can be understood in the opposite manner. Cold advection is feasible over East Asia during the negative phase of AO, EA/WR, WP, and ENSO. As discussed in Figure 5, northerly

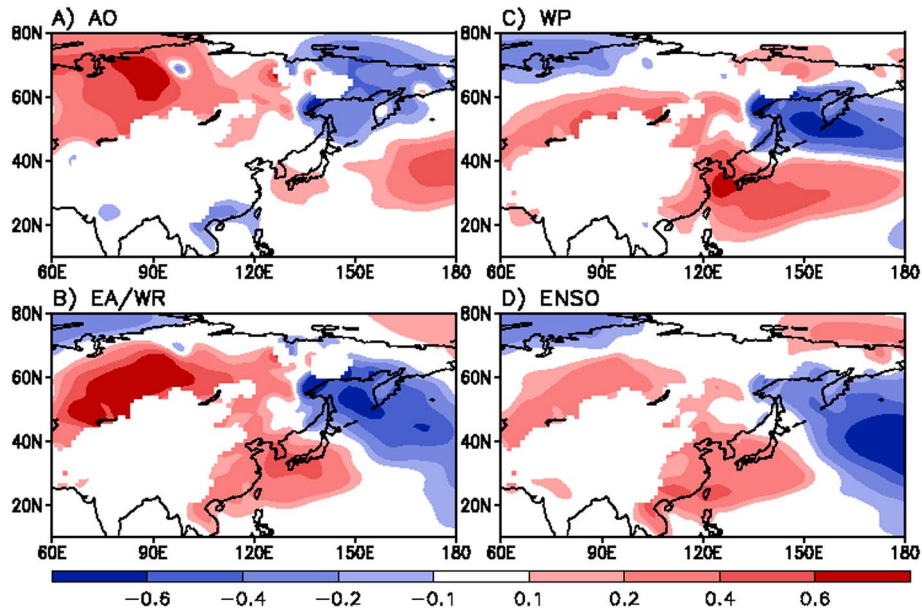


Figure 6. Distribution of the advective temperature change ($-V_{Tel} \cdot \nabla T_{Cli}$) Kd^{-1} by 850 hPa atmospheric circulation linked to each teleconnection. V_{Tel} indicates the horizontal winds linked to each teleconnection, and T_{Cli} represents the climatological temperatures.

flow associated with large-scale cyclonic circulation is favored during the negative teleconnection phases over East Asia. The northerly flow may contribute to cold advection toward East Asia.

[24] Upper level atmospheric structures in response to each teleconnection are also investigated. Figure 7 shows the distribution of upper level jet anomalies in response to each teleconnection. The most pronounced identical feature among the figure panels is the weakening (intensification) of the upper level jet over midlatitude East Asia during the positive (negative) phase of the teleconnections. *Yang et al.*

[2002] also found that the East Asian jet weakening (intensification) is linked to warmer (colder) winter condition. While the jet intensity change over continental East Asia is found at $30^{\circ}N-45^{\circ}N$ for the AO, EA/WR, and ENSO cases, WP case shows the jet intensity change in the Pacific. This pattern in the WP case is linked to the strong dipole structure of pressure anomalies which are typically found in the WP pattern.

[25] Weakening of the jet intensity during the positive phase of teleconnection is related to the easterly anomaly that counteracts the existing climatological of the westerly jet. Upper level easterly or southeasterly anomalies over

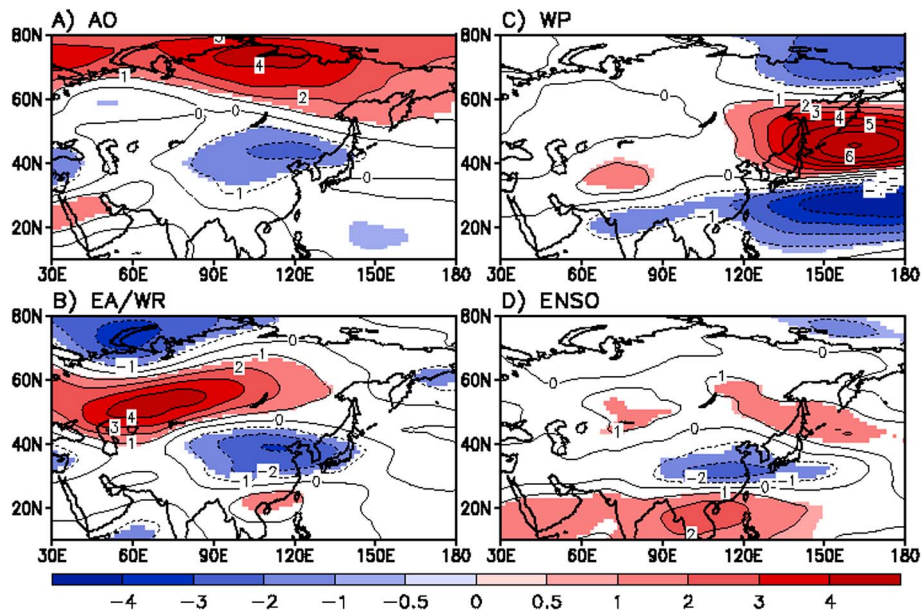


Figure 7. Distribution of the regressed zonal wind anomalies [$m s^{-1}$] at 300 hPa onto each teleconnection. Winds statistically significant at 10% level are shaded.

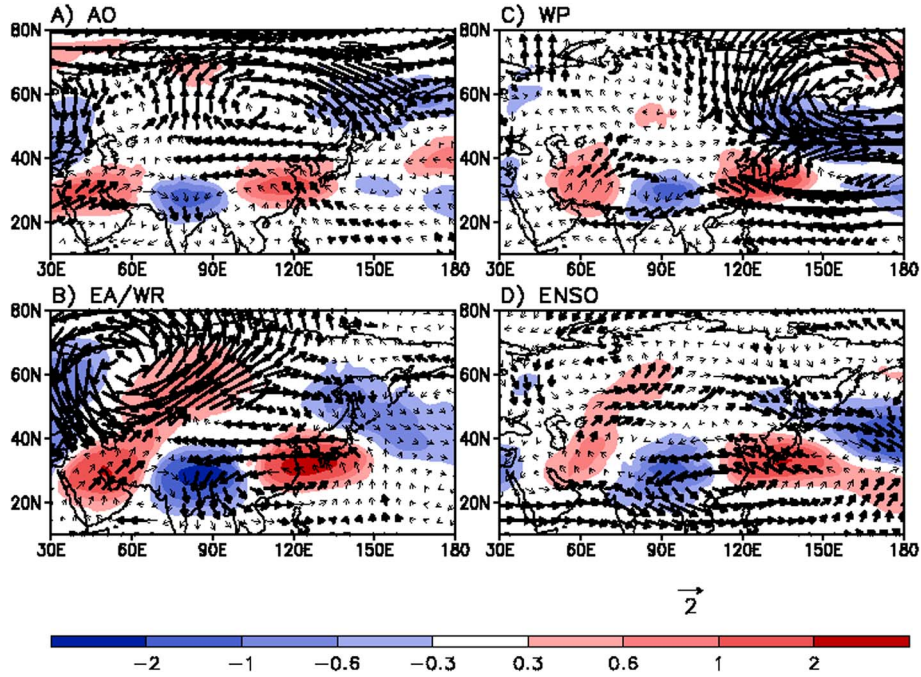


Figure 8. Distribution of the regressed 300 hPa atmospheric circulations [m s^{-1}] and advective temperature changes [K d^{-1}] of each teleconnection. Wind vectors statistically significant at 10% level are plotted with thicker lines.

midlatitude East Asia are evident in Figure 8. Shadings represent the advective temperature change by the impact of the upper level circulation anomalies. It clearly shows that they not only weaken the midlatitude westerly jet but also contribute to warm advection toward midlatitude East Asia, centered in eastern China, Korea, and Japan. This strong warm advection is found in all four teleconnection events, with relatively stronger advection in the case of EA/WR case. As well as the lower level case discussed in Figure 6, the upper level temperature advection of EA/WR and WP is comparable to that of AO, suggesting an important role of EA/WR and WP in resolving winter climates over East Asia. The circulation structures and corresponding temperature advection for the case of negative teleconnection phase can be understood in the opposite manner. Westerly and northwesterly anomalies that enhance the midlatitude westerly jet are expected over East Asia. Those wind anomalies contribute to cold advection toward midlatitude East Asia by transporting the continental cold air mass from the higher latitudes.

[26] The wave activity flux (WAF) patterns for the four teleconnection events were examined to identify the source and propagation of wave activity which influences the East Asian winter climate. Following *Plumb* [1985], the stationary WAF is given as

$$F_s = p \cos \varphi \begin{pmatrix} v^2 - \frac{1}{2\omega \sin \varphi} \frac{\partial(v'\Phi')}{\partial \lambda} \\ -u'v' + \frac{1}{2\omega a \sin 2\varphi} \frac{\partial(u'\Phi')}{\partial \lambda} \\ \frac{2\omega \sin \varphi}{S} \left[v'T' - \frac{1}{2\omega a \sin 2\varphi} \frac{\partial(T'\Phi')}{\partial \lambda} \right] \end{pmatrix}$$

where the variables (u , v), p , T , Φ , and S in the equation represent zonal and meridional wind, pressure, temperature,

geopotential height, and static stability, respectively, and where λ and φ represent longitude and latitude. The constant ω is the Earth's rotation rate ($=7.292 \times 10^{-5} \text{ rad s}^{-1}$) and a is the radius of the Earth. The prime denotes the deviation from the zonal mean at each latitude and height. $S = \frac{\partial \hat{T}}{\partial z} + \frac{\kappa \hat{T}}{H}$ is the static stability; caret indicates an areal average over the Northern Hemisphere; κ ($=287/1004 \text{ J K}^{-1} \text{ kg}^{-1}$) is the ratio of gas constant to specific heat at constant pressure; H is the constant-scale height.

[27] Horizontal WAF at 300 hPa is plotted in Figure 9. WAF usually propagates eastward, which is consistent with *Hoskins and Karoly* [1981]. The wave train spreading toward East Asia across the Eurasian region is clearly found in the EA/WR case (Figure 9b). It demonstrates the substantial role of EA/WR teleconnection in influencing the East Asian winter climates by wave propagation across the ridge-trough patterns shown in Figure 1. Upper level westerly anomalies and circulation anomalies in Figures 7b and 8b are also the results of the ridge-trough patterns across the Eurasian region. Compared with EA/WR, WAF for AO tends to propagate along the high-latitudes. It can be understood that the impact of AO on the East Asian winter climates tends to come from higher latitudes north of midlatitude East Asia. Figures 7a and 8a are consistent with this argument in that the location of pronounced height and circulation anomalies is found north of midlatitude East Asia. Compared with the AO, the impact of EA/WR appears to propagate south-eastward from the western Russia in the type of stationary wave train (Figures 7b, 8b, and 9b). The strong WAF for the WP case tends to be confined over the Pacific. *Yang et al.* [2002] discuss that the enhanced jet along the East Asian storm track is important to have sufficient WAF cross the Pacific to reach North America. The WAF for ENSO in

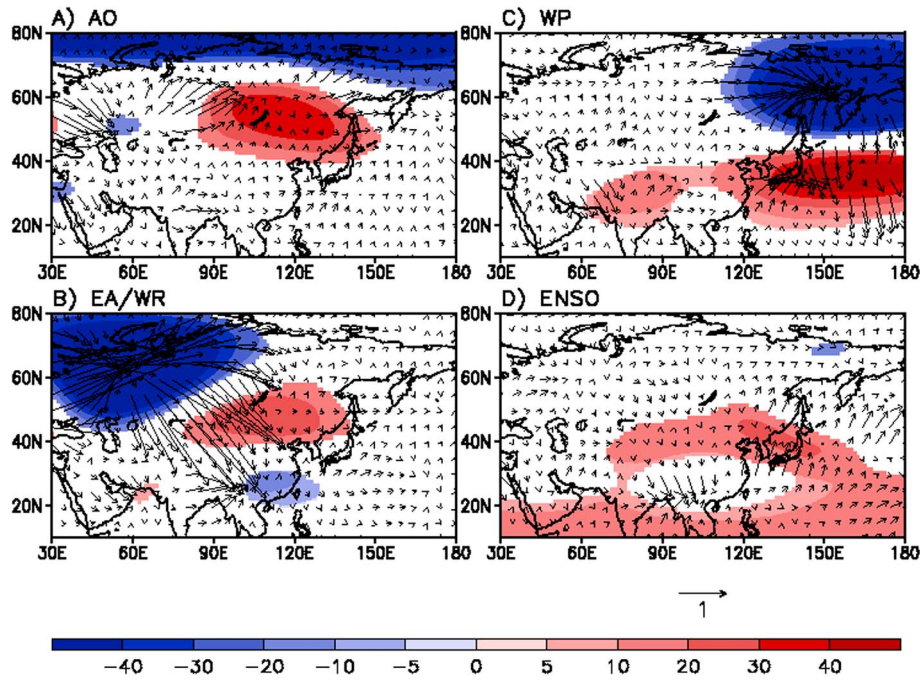


Figure 9. Distribution of the wave activity fluxes [$\text{m}^2 \text{s}^{-2}$] and geopotential height anomalies [m] at 300 hPa associated with each teleconnection. Geopotential height anomalies statistically significant at 10% level are shaded.

Figure 9d indicates that the impact of ENSO in terms of wave propagation comes from the subtropical western Pacific. Karoly *et al.* [1989] and Yang *et al.* [2002] address the fact that ENSO is characterized by the changes in meridional propagation of WAF over the tropical Pacific, but that weaker signals exist in the extratropics.

6. The Contribution of Each Teleconnection to the Temperature Anomalies for the Selected Winters

[28] Previous sections delineate the general features of the impact of each teleconnection on the East Asian winter climate, based on averaged over 33 winters (1979/1980–2011/2012). In this section, we diagnose the impact of each teleconnection for individual years. To do this, we first reconstruct the 2 m temperature anomaly data over 33 winter periods with respect to the leading four teleconnections. Four sets of reconstructed data are produced by linear combination of the regressed temperature pattern for each teleconnection and its index time series. The resulting four data sets represent the interannual variation of the temperature anomalies by the impact of each teleconnection.

[29] Temperature distributions for four selected winters are examined in Figures 10 through 13. Figure 10 represents the result for 2009/2010, which is representative of a strong negative AO (-3.4) according to the National Oceanic and Atmospheric Administration (NOAA) observation [http://www.cpc.ncep.noaa.gov/products/precip/CWlink/daily_ao_index/monthly_ao.index.b50.current.ascii.table], and El Niño (Southern Oscillation index (SOI): -1.8) [<http://www.cpc.ncep.noaa.gov/data/indices/soi>]. East Asia is known to show a typically cold winter response to negative AO [Jeong and Ho, 2005; Park *et al.*, 2010] and a warm winter response to El Niño [Zhang *et al.*, 1997], indicating that two opposite impacts

coexisted over East Asia in the winter of 2009/2010 (Figures 10a and 10d). The comparison of the magnitudes of temperature anomalies indicates a stronger impact of AO than El Niño over East Asia. According to the National Oceanic and Atmospheric Administration (NOAA)/National Centers for Environmental Prediction (NCEP) report, this strong negative AO lasted throughout the 2009/2010 DJF period. This negative AO impact contributes substantially to severe cold winter over Eurasia, including that in far eastern Asia (Figure 10a). Negative temperature anomaly values over East Asia range from -2 K to -1 K . The EA/WR, which is in the same phase with the negative AO in 2009/2010 winter, also has a cooling impact over East Asia (Figure 10b). Temperature anomalies of the impact of WP are scarcely found throughout the winter of 2009/2010, as the WP is in near neutral phase (Figure 10c). ENSO is in the positive phase that has a warming impact over East Asia (Figure 10d). However, positive ENSO impact (i.e., El Niño) does not appear to be stronger than the impact of negative AO or EA/WR. Temperature distributions in Figures 14a and 14e, which reflect the combined effect of the four leading teleconnections, do not show positive temperature anomalies at all over Mongolia, northeastern China, of Korea due to the weaker impact of El Niño as compared to the negative AO impact. The observed temperature anomalies in Figure 14e indicate severely cold winter over East Asia except in central to southern China, where a warm winter would be expected under such circumstances due to the impact of El Niño.

[30] We next examined the winter of 1997/1998, which is recorded as the strongest El Niño year within the past three decades. Figure 11 illustrates the contribution to the winter temperature by each teleconnection. EA/WR, WP, and ENSO are in the positive phase and play a role in the advection of warm air toward East Asia (Figures 6b–6d and 11b–11d).

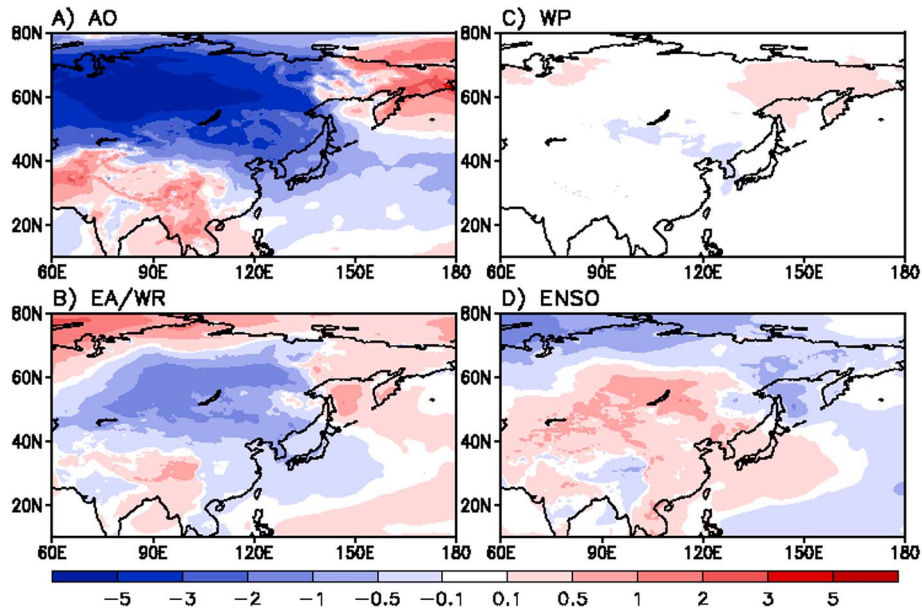


Figure 10. Distribution of 2 meter air temperature anomalies [K] resulting from the impact of each teleconnection for winter 2009/2010 DJF.

The observed temperatures over East Asia distributed in Figure 14f are above average due to the warming effect of these teleconnection patterns. In contrast, AO in negative phase plays a role in inducing cold winter over the region (Figure 11a). In contrast to the winter of 2009/2010 (Figure 10), the cooling impact by AO alone is not stronger than the combined warming impact of the other three teleconnections in the winter of 1997/1998, resulting in a warmer than average winter.

[31] We additionally examined the winter of 2011/2012 as the recent winter which represented the different feature of combination of each teleconnection impact compared with the previous two winter cases. The 2011/2012 winter is

characterized by weak La Niña (SOI: 2.2) and dramatic phase change of AO in the middle of season [2.22 (December), -0.22 (January), and -0.04 (February)] based on the index data released from NOAA. Positive AO dominates until early January and turns to the negative phase in late January and early February, causing a subseasonal cold spell over the Northern Hemispheric midlatitudes. The East Asian region also experiences this subseasonal cold period in February, which is in contrast to the first two warm months [<http://www.ncdc.noaa.gov/sotc/global/2012/2>]. However, seasonally averaged AO is recorded as positive (1.96). The 2 m air temperature anomalies associated with the seasonally averaged AO signature are positive as shown in Figure 12a.

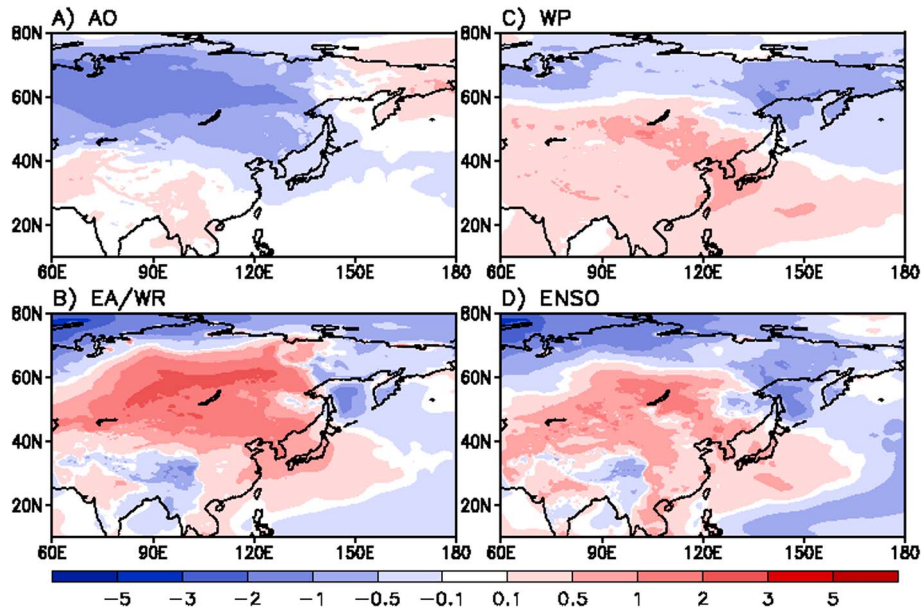


Figure 11. Same as Figure 10 but for the winter period of 1997/1998.

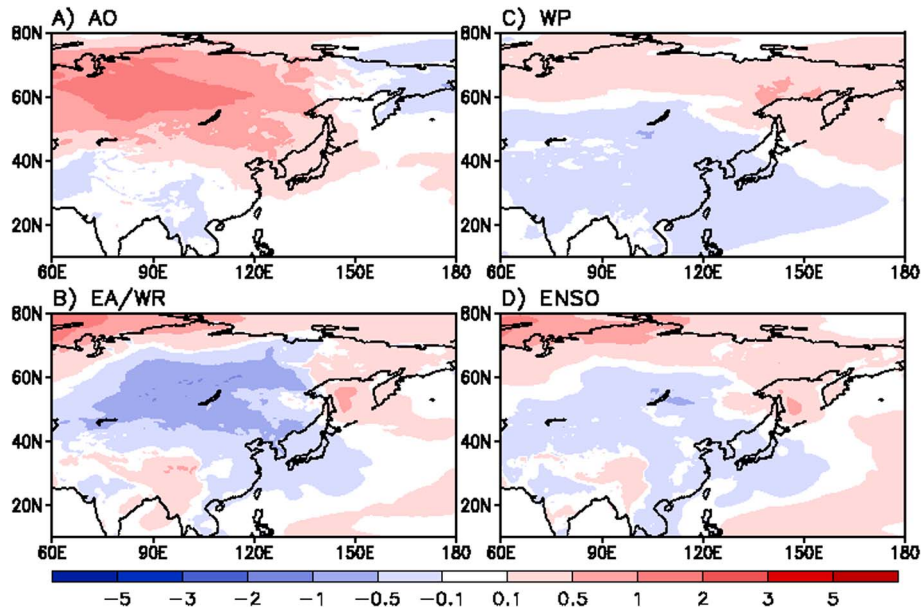


Figure 12. Same as Figure 10, but for the winter of 2011/2012.

EA/WR is in the strong negative phase, making a significant contribution to cold winter over East Asia (Figure 12b). The WP impact is weak, making a small contribution toward colder winters (Figure 12c). Also, the weak negative ENSO signal (i.e., La Niña) plays a slight role in causing cold temperature distribution over East Asia (Figure 12d). The resulting observed temperature anomaly over East Asia by the combined effect of the four teleconnections is negative, as seen in Figure 14g. The negative phase of EA/WR appears to be more responsible for colder winters than normal and is followed by smaller contributions by WP and ENSO.

[32] While the combined effect of the teleconnections in 2011/2012 is rather complicate, 2010/2011 winter is an easy case to predict seasonal temperature as all four teleconnections

are characterized by a negative phase. Figure 13 clearly shows that temperature anomalies by the impact of each teleconnection are generally negative over the East Asian region, indicating cold winter as it is confirmed in Figures 14d and 14h.

[33] As discussed in Figures 10 through 13, the diverse ways of contribution of teleconnection patterns leads to different temperature patterns each year across the Eurasian domain. *Hamilton* [1988] discussed that the actual midlatitude circulation anomalies show a great deal of variability among individual ENSO years, possibly due to the interference of the impact of the other large-scale patterns. The left panel in Figure 14 represents the regressed 2 m air temperature anomaly distributions retrieved from the combined

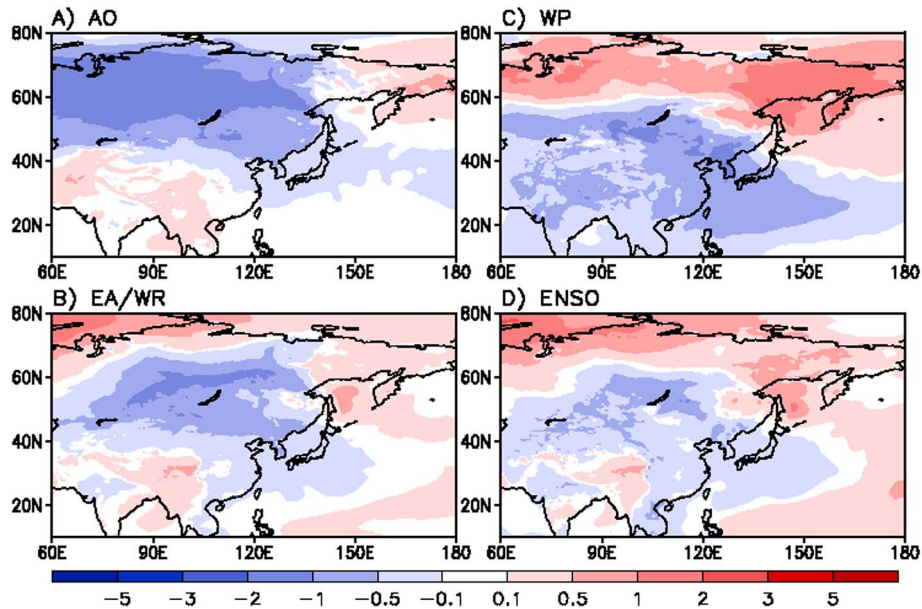


Figure 13. Same as Figure 10, but for the winter of 2010/2011.

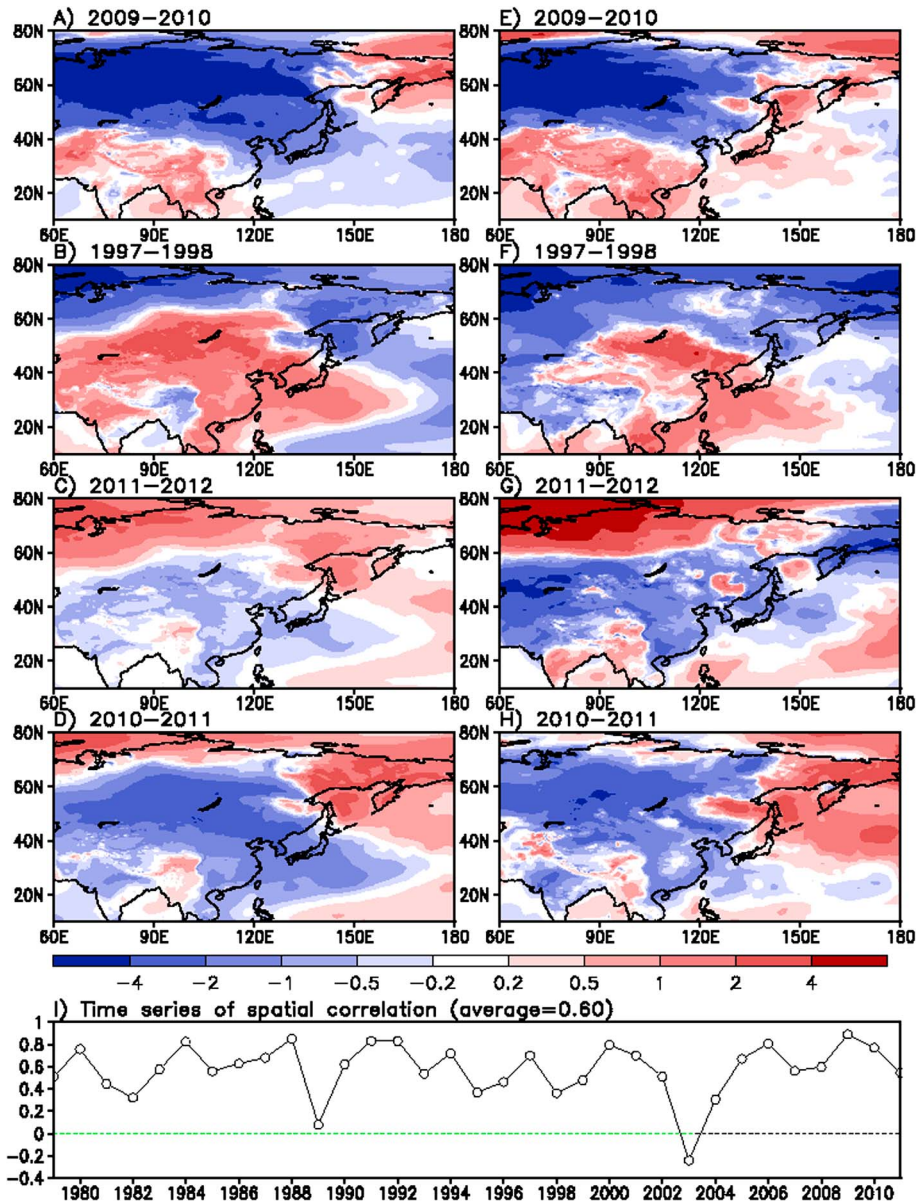


Figure 14. (Left) Distribution of 2 m air temperature anomalies [K] resulting from the combined effect of the four leading teleconnections. Four winters: 2009/2010, 1997/1998, 2011/2012, and 2010/2011 are plotted. (Right) Observed 2 meter air temperature anomalies for the corresponding winters. Time series on the bottom panel represent the spatial correlation coefficient between the reconstructed temperature and observed temperature each year. Spatial domain for calculating correlations is 90°E–180°E, 10°N–80°N.

effect of the major four teleconnection patterns. The anomalies are plotted for the four different winters delineated in Figures 10 through 13. The right column in Figure 14 represents the distribution of the observed 2 m air temperature anomaly for the corresponding winters. It can be seen from this figure that the temperature anomalies resulting from the combined effect of the major four teleconnections (Figure 14, left panel) are quite consistent with the distribution of the observed temperature anomalies (Figure 14, right column). As discussed in Figure 10, the winter of 2009/2010 was affected more by strong negative AO and EA/WR impact than by ENSO, leading to a colder winter over East Asia, primarily north of 40°N (Figures 14a and 14e). Positive temperature anomalies over central to southern

China can be understood by the combined effect of AO, EA/WR, and El Niño (please see Figures 10a, 10b, and 10d). In contrast, the winter of 1997–1998 is influenced by a strong El Niño phase. In addition to the impact of El Niño impact, the positive impacts of EA/WR and WP also contribute to the positive temperature anomalies over East Asia (Figures 11b, 11c, and 11d). Their combined effect appears stronger than the cooling impact by AO shown in Figure 11a, resulting in a wide area of positive temperature anomalies over East Asia including China, Mongolia, Korea, and Japan (Figure 14b). Comparison in the temperature anomaly distribution between Figures 14b and 14f provides strong evidence that the combined effect of the four leading teleconnections explains the observed temperature anomalies

over the domain. The 2011/2012 winter also clarifies that the observed temperature anomalies can be reasonably well explained by the combined effect of the four leading teleconnections (Figures 14c and 14g). Distribution of the negative temperature anomalies over East Asia is a consequence of the cooling impact of the negative EA/WR, followed by a small contribution from La Niña and WP (Figures 12b–12d). The temperature distribution for 2010/2011 winter is plotted in Figures 14d and 14h. All four teleconnection patterns show a negative phase during this winter (Figure 13). As a result, the East Asian region exhibits a cold winter response to the impact of negative AO, EA/WR, WP, and La Niña (Figures 14d and 14h).

[34] Four winter examples above show a great explanation of the East Asian winter temperatures by the dominant four teleconnections. However, we also found exceptional winters, when temperatures are not well reproduced by the combined effect of the four teleconnections. Winters in 1989–1990 and 2003–2004 show near zero or even negative spatial correlations (Figure 14i), indicating poor representation of the observed temperature anomalies by the reconstructed anomalies. Our reconstruction by adding higher modes that appear to represent Scandinavian pattern [Wallace and Gutzler, 1981] and East Atlantic (EA) pattern [Washington *et al.*, 2000] significantly increases the correlation for 2003–2004 winter up to ~ 0.4 . It is suggested that, although the four teleconnections explain substantial portion of winter temperatures for the past 33 winters (averaged spatial corr. = 0.6, Figure 14i), there seem to be another few teleconnections that should receive attention to fully explain the East Asian winter temperature variability.

7. Concluding Remarks

[35] The present study investigated the impact of the leading large-scale teleconnections on winter temperature variation over East Asia. MERRA reanalysis data were used for the past 33 winters (DJF) from 1979/1980 through 2011/2012. The large-scale patterns, AO, EA/WR, WP, and ENSO are identified as the first four leading modes that significantly explain the interannual variation of winter temperatures over East Asia. Regression of 2 m air temperatures onto the large-scale circulation patterns exhibits a positive temperature anomaly distribution during the positive phase of their patterns whereas the negative anomaly during the negative phase. Many previous studies address the fact that the East Asian winter climate is substantially determined by the impact of AO and ENSO. The present study, however, realizes that temperatures in the East Asian region are also significantly influenced by WP and EA/WR. The average impact of ENSO turns out to be relatively weaker than that for the other three teleconnections over the last 33 winters. The contribution of EA/WR and WP to East Asian temperature anomalies is often comparable to the impact of AO. The analysis clearly demonstrates that main surface temperature anomalies associated with positive phases of the EA/WR reflect above-average temperatures over East Asia, along with below-average temperatures over large portions of western Russia. The positive WP pattern that consists of a north-south dipole of anomalies, reflecting the variations of the location and strength of the jet stream entrance over East Asia, has a warming impact over East Asia and a cooling

impact over high-latitudes of Russia. Compared to AO, EA/WR, WP, and ENSO show larger portions of the contribution of advective process to determine temperature distributions over East Asia. Examination of the WAF at upper level reveals that a stationary wave tends to propagate eastward along the high latitudes in the case of AO, while the wave from the western Russia propagates southeastward into mid-latitude East Asia in the case of EA/WR. Difference in the WAF between the two teleconnection events indicates that the impact of AO toward midlatitude East Asia tends to come from the circulation and height anomalies at higher latitudes north of midlatitude East Asia. In the case of EA/WR, the impact tends to come from northwest of midlatitude East Asia in the form of a stationary wave train.

[36] The present study also evaluates the contribution of the leading large-scale teleconnections to the East Asian winter temperatures for the selected years. It reveals that the aspect of combined teleconnections is different each year. Particularly, the most dominant teleconnection pattern resolving the regional temperature anomaly is not necessarily the same throughout all years. This, in turn, indicates that no teleconnection pattern could be considered to be the consistently most dependable for seasonal predictions every year. A more elaborate examination of the individual teleconnection patterns, not limited to the conventional reliance on one or two signals, such as AO and ENSO, would be desirable for more accurate seasonal predictions of the East Asian winter climate.

[37] One of the limitations of the present study is that we assume the spatial structure of atmospheric responses between the positive and negative phases of each teleconnection to be nearly symmetric. In addition, we found that combined effect of the four teleconnection is still insufficient to completely reproduce the observed winter temperature variability over East Asia. Nonetheless, the results are expected to be useful to convey the improved general understanding of the atmospheric response to the dominant teleconnections and their contribution to East Asian winter temperatures.

[38] **Acknowledgments.** This research was supported by the Scholar Research Grant of Keimyung University in 2012.

References

- Barnston, A. G., and R. E. Livezey (1987), Classification, seasonality and persistence of low-frequency atmospheric circulation patterns, *Mon. Weather Rev.*, *115*, 1083–1126.
- Barnston, A. G., R. E. Livezey, and M. S. Halpert (1991), Modulation of Southern Oscillation-Northern Hemisphere mid-winter climate relationships by the QBO, *J. Clim.*, *4*, 203–217.
- Bojariu, R., and G. Reverdin (2002), Large-scale variability modes of freshwater flux and precipitation over the Atlantic, *Clim. Dyn.*, *18*, 369–381, doi:10.1007/s003820100182.
- Chen, T.-C., W.-R. Huang, and J.-H. Yoon (2004), Interannual variation of the East Asian cold surge activity, *J. Clim.*, *17*, 401–413.
- Gershunov, A., and T. P. Barnett (1998), ENSO influence on intraseasonal extreme rainfall and temperature frequencies in the contiguous United States: Observations and model results, *J. Clim.*, *11*, 1575–1586.
- Griffiths, M. L., and R. S. Bradley (2007), Variations of twentieth-century temperature and precipitation extreme indicators in the northeast United States, *J. Clim.*, *20*, 5401–5417.
- Hamilton, K. (1988), A detailed examination of the extratropical response to tropical El Niño/Southern Oscillation events, *Int. J. Climatol.*, *8*, 67–86.
- Higgins, R. W., A. Leetmaa, and V. E. Kousky (2002), Relationships between climate variability and winter temperature extremes in the United States, *J. Clim.*, *15*, 1555–1572.

- Horel, J. D. (1981), A rotated principal component analysis of the interannual variability of the Northern Hemisphere 500mb height field, *Mon. Weather Rev.*, *109*, 2080–2092.
- Horel, J. D., and J. M. Wallace (1981), Planetary-scale atmospheric phenomena associated with the Southern Oscillation, *Mon. Weather Rev.*, *109*, 813–829.
- Hoskins, B. J., and D. J. Karoly (1981), The steady linear response of a spherical atmosphere to thermal and orographic forcing, *J. Atmos. Sci.*, *38*, 1179–1196.
- Jeong, J.-H., and C.-H. Ho (2005), Changes in occurrence of cold surges over East Asia in association with Arctic Oscillation, *Geophys. Res. Lett.*, *32*, L14704, doi:10.1029/2005GL023024.
- Karoly, D. J., R. A. Plumb, and M. Ting (1989), Examples of the horizontal propagation of quasi-stationary waves, *J. Atmos. Sci.*, *46*, 2802–2811.
- L'Heureux, M., A. Butler, B. Jha, A. Kumar, and W. Wang (2010), Unusual extremes in the negative phase of the Arctic Oscillation during 2009, *Geophys. Res. Lett.*, *37*, L10704, doi:10.1029/2010GL043338.
- Lim, Y.-K., and S. D. Schubert (2011), The impact of ENSO and the Arctic Oscillation on winter temperature extremes in the southeast United States, *Geophys. Res. Lett.*, *38*, L15706, doi:10.1029/2011GL048283.
- Linkin, M. E., and S. Nigam (2008), The North Pacific Oscillation-West Pacific teleconnection pattern: Mature-phase structure and winter impacts, *J. Clim.*, *21*, 1979–1997.
- Meehl, G. A., C. Tebaldi, H. Teng, and T. C. Peterson (2007), Current and future U.S. weather extremes and El Niño, *Geophys. Res. Lett.*, *34*, L20704, doi:10.1029/2007GL031027.
- Mo, K. C., and R. E. Livezey (1986), Tropical-extratropical geopotential height teleconnections during the northern hemisphere winter, *Mon. Weather Rev.*, *114*, 2488–2515.
- Park, T.-W., C.-H. Ho, S. Yang, and J.-H. Jeong (2010), Influences of Arctic Oscillation and Madden-Julian Oscillation on cold surges and heavy snowfalls over Korea: A case study for the winter of 2009–2010, *J. Geophys. Res.*, *115*, D23122, doi:10.1029/2010JD014794.
- Park, T.-W., C.-H. Ho, and S. Yang (2011), Relationship between the Arctic Oscillation and cold surges over East Asia, *J. Clim.*, *24*, 68–83.
- Plumb, R. A. (1985), On the three-dimensional propagation of stationary waves, *J. Atmos. Sci.*, *42*, 217–229.
- Rienecker, M. M., et al. (2011), MERRA-NASA's modern-era retrospective analysis for research applications, *J. Clim.*, *24*, 3624–3648.
- Thompson, D. W. J., and J. M. Wallace (1998), The Arctic oscillation signature in the wintertime geopotential height and temperature fields, *Geophys. Res. Lett.*, *25*(9), 1297–1300, doi:10.1029/98GL00950.
- Wallace, J. M., and D. S. Gutzler (1981), Teleconnections in the geopotential height field during the Northern Hemisphere winter, *Mon. Weather Rev.*, *109*, 784–812.
- Wang, X., C. Wang, W. Zhou, D. Wang, and J. Song (2011), Teleconnected influence of North Atlantic sea surface temperature on the El Niño onset, *Clim. Dyn.*, *37*, 663–676, doi:10.1007/s00382-010-0833-z.
- Washington, R., A. Hodson, E. Isaksson, and O. Macdonald (2000), Northern hemisphere teleconnection indices and the mass balance of Svalbard glaciers, *Int. J. Climatol.*, *20*, 473–487.
- Yang, S., K.-M. Lau, and K.-M. Kim (2002), Variations of the East Asian jet stream and Asian-Pacific-American winter climate anomalies, *J. Clim.*, *15*, 306–325.
- Zhang, Y., K. R. Sperber, and J. S. Boyle (1997), Climatology and interannual variation of the East Asian winter monsoon: Results from the 1979–95 NCEP/NCAR reanalysis, *Mon. Weather Rev.*, *125*, 2605–2619.